scientific reports

OPEN

On the need to integrate interannual natural variability into coastal multihazard assessments

I. Odériz[1]✉, I. J. Losada[1], R. Silva[2] & N. Mori[3,4]

The co-occurrence of multiple hazards can either exacerbate or mitigate risks. The interrelationships between multiple hazards greatly depend on the spatiotemporal scale and can be difficult to detect from large to local scales. In this paper, we identified coastal regions worldwide where the leading tropical (El Niño-Southern Oscillation, ENSO) and polar (Arctic Oscillation, AO; Southern Annular Mode, SAM) modes of climate variability simultaneously modify the seasonal conditions of multiple hazards, including the near-surface wind speed and swell and wind-sea wave powers. We classified the results at the national and municipal levels, with a focus on multiple hazards simultaneously occurring in space and time. The results revealed that the ENSO modulates multiple hazards, affecting approximately 40% of coastal countries, while the polar annular modes affect approximately 30% of coastal countries. The ENSO induced a greater diversity of multiple hazards, with Asian countries (e.g., Indonesia experienced increases of + 2% in wind and + 7% in swell) and countries in the Americas (e.g., Peru exhibited increases of + 1.5% in wind and + 6% in wind-sea) the most notably affected. The SAM imposed a greater influence on swells in the eastern countries of ocean basins (+ 2.5% in Chile) than in other countries, while the influence of the AO was greater in Norway and the UK (+ 12% for wind-sea and 8% for swell). Low-lying islands exhibited notable variations in pairwise hazards between phases and seasons. Our results could facilitate the interpretation of multihazard interactions and pave the way for a wide range of potential implementations of different coastal industries.

Keywords Multihazard, Winds, Ocean waves, AO, SAM, ENSO

Climate trends and natural variability greatly impact the global economy. In Europe, weather variability is associated with a cost of more than € 560 billion Euros per year[1], while in the United States, the estimated cost in 2008 accounted for approximately 3.4% of the gross domestic product[2]. At the interannual scale, the El Niño-Southern Oscillation (ENSO) affects economic growth in countries with climate-sensitive sectors, increasing their vulnerability[3]. This is the case for countries with coastal areas dependent on tourism, marine energy and the port industry[4].

From a climate dynamics perspective, it is widely considered that natural climate variability modes (hereinafter referred to as climate modes) can modulate single hazards—wind[4] and waves[5–8]. During the positive phase of the Southern Annular Mode (SAM), ocean waves increase in wave height[5,8] and energy[6,9] in the Southern Ocean. The positive phase of the ENSO, referred to as El Niño, is associated with intensified extratropical winds[10] and ocean waves in the central North Pacific[11]. The positive phase of the Arctic Oscillation (AO) is associated with increased wind velocity and wave height levels in the North Atlantic[6,12].

Winds and waves are responsible for several coastal impacts, Fig. 1a. Winds can lead to maritime disruptions[13], variations in energy production[14] and damage to energy infrastructure and buildings[15]. Wind setup is also a driver of storm surge that can cause flooding[16]. Waves, on the other hand, influence wave energy supply, port operability, damage to infrastructure, coastal erosion and flooding[17], depending on wave direction and on the type of wave system, swell and wind-sea[18–21]. However, to date, interannual variations have not been recognized as drivers of flooding in the same way as long-term variations in mean and total sea levels[22], nor are long-term wind[23] and wave variabilities[24] considered for investments in the energy[23] and insurance industries[25]. Linkages between the

[1]IHCantabria - Instituto de Hidráulica Ambiental de La Universidad de Cantabria, Santander, Spain. [2]Instituto de Ingeniería, Universidad Nacional Autónoma de México, Mexico City, Mexico. [3]Disaster Prevention Research Institute, Kyoto University, Kyoto, Japan. [4]Swansea University, Swansea, UK. ✉email: itxaso.oderiz@unican.es

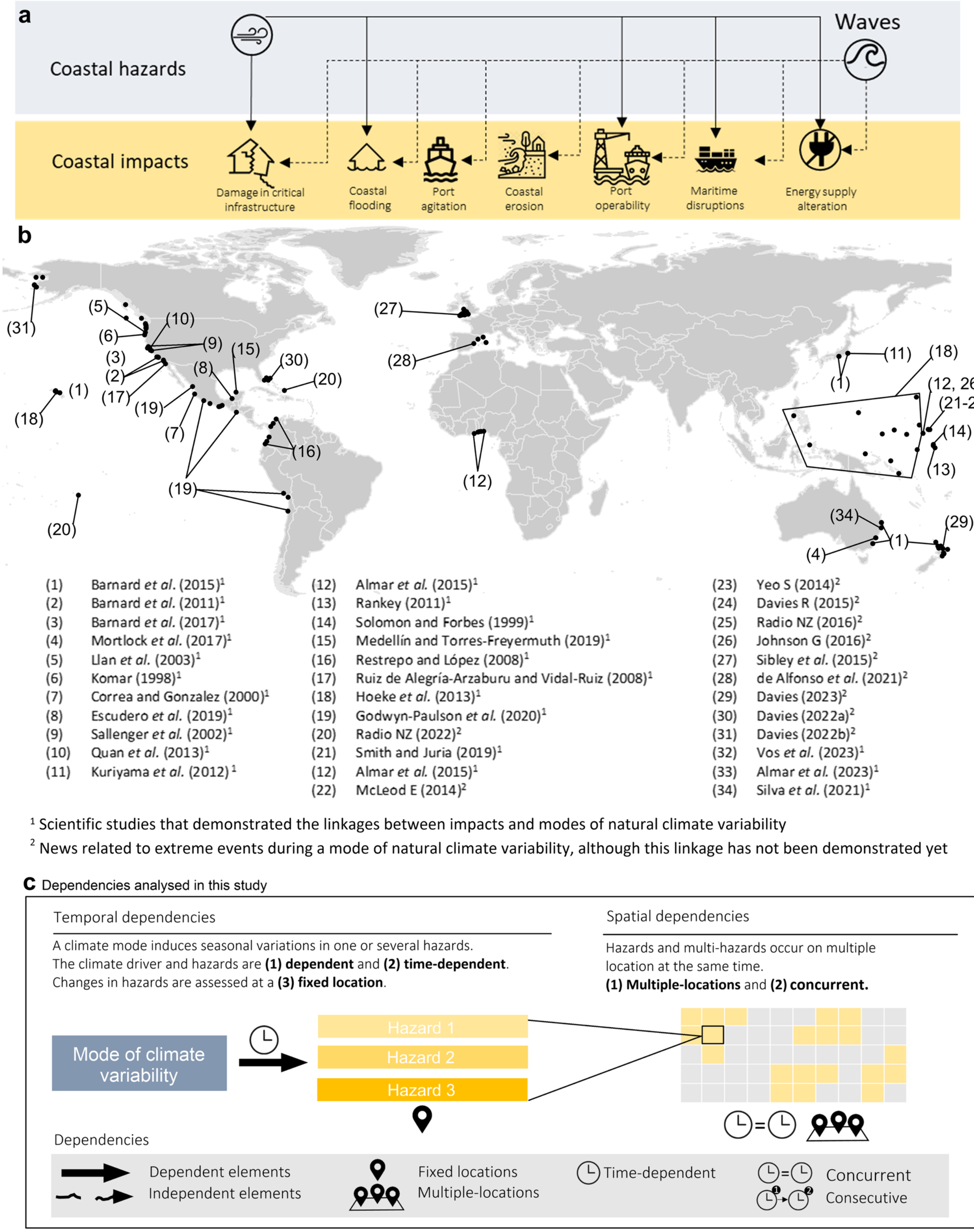

Figure 1. **(a)** Scheme of coastal impacts related to winds and waves. **(b)** A catalogue of historical impacts related to modes of climate variability. It includes scientific studies that demonstrated the linkage between impacts and climate modes, as well as news related to extreme events during a mode of climate variability, although this linkage has not been demonstrated yet. References of this figure can be found in Supplementary Table S1. **(c)** Scheme of temporal and spatial dependencies analysed in this study.

above climate modes and coastal impacts have been demonstrated primarily for explaining exceptional extreme events[26] or in a limited number of regions with monitoring records[27], leaving many regions worldwide underrepresented (Fig. 1b).

The focus of existing research is multihazard[30] analysis because the dependencies between multiple hazards can either exacerbate or mitigate risks[28]. Multihazards are defined by Sendai Fremework[29] as multiple major hazards with potential interrelated effects over time. In response to a series of consecutive disasters, the European Union has recommended the evaluation of risks over longer timescales, extending beyond the immediate post-disaster recovery period[30]. Examples shown in Fig. 1b illustrate how climate modes can modify the seasonal climate worldwide, leading to changes in storminess and contributing to coastal impacts.

In coastal areas, despite the fact that the long-term variation in single hazards induced by climate modes has been studied in depth, neither the anomalies of multiple hazards derived from the natural variability nor the linkages between various climate modes and coastal impacts have been fully explained on a global scale. As a preliminary step, in this work, we aimed to identify coastal regions worldwide at the national and municipal scales, where the leading tropical (ENSO) and polar (AO and SAM) climate modes[31,32] modify seasonality of multiple hazards by considering the near-surface wind speed and wave power. Regarding the latter, wind-sea and swell wave powers were differentiated. We started by analysing the temporal dependencies between seasonal hazard variations and climate modes. Then, we evaluated spatial dependencies at the local and national scales.

Climate modes and multihazard dependencies

Based on the literature[28,30,33–35], we synthetized the interrelationships between multiple hazard elements, as shown in Fig. 1c. Following the typology proposed by Zscheischler et al.[28], the elements of the ENSO, AO and SAM were identified as modulators—climatic drivers that influence the frequency and location of hazards. In this paper, the hazards that trigger coastal impacts are waves and winds. The dependencies between the elements were categorized into (1) time lags between events (e.g., concurrent or consecutive), (2) spatial dependencies (which can involve fixed or multiple regions), and (3) relationships between the elements (which can depend on whether a given element is caused or modulated by another element or not). In this study, we analysed the seasonal variations (time-dependent) in one or multiple hazards at fixed locations induced by a given climate mode, where the climate mode and hazards are dependent. Subsequently, the co-occurrences of these multiple hazards in multiple regions were analysed. For the latter we have used coastal municipalities as work units. These are the geographic area with local governments, which practitioners can understand better the interaction of impacts and consequences in a spatial interaction.

We analysed a total of nine hazards, combining wave power and wind speed, depending if waves or winds belong to a specific climate regime. Additionally, we distinguished between wind-sea and swell wave powers. Thus, hazards were classified in climates. For this, we used the dataset of Odériz et al.[6], which consists of a classification of global winds and waves from 1979 to 2018 by applying a *dynamic clustering* algorithm[6], with parameters from ERA5 reanalysis data and subsequently referred to as wind (W, E, and S), wind-sea (W, E, and S), and swell (W, E, and S). It should be noted that the terms speed and wave power are not used in this paper, as at all times, wind denotes the wind speed, and wind-sea and swell denote the corresponding wave powers.

We identified the phases of climate modes using climate indices from the National Weather Service Climate Prediction Center of the National Oceanic and Atmospheric Administration (NOAA), namely, the monthly AO index (for the Arctic Oscillation), monthly SAM index (for the Southern Annular Mode), and multivariate ENSO index version 2 (MEI.v2) (for the El Niño-Southern Oscillation). The positive/negative phases of these climate modes were expressed as ENSO + /ENSO-, AO + /AO-, and SAM + /SAM-. The seasons were classified as follows: December, January, and February (DJF), March, April, and May (MAM), June, July, and August (JJA), and September, October, and November (SON).

For each hazard, we calculated composite anomalies by averaging hazard anomalies under a specific climate (W, S, and E) and season during a given climate mode phase. Seasonal composite anomalies contribute to identifying when and where these hazards occur at more or less intensely than during an average season. Only significative values were considered. Throughout this paper, composite anomalies are expressed as percentages of the anomalies mean compared to the average seasonal value for a given location. A positive (negative) value indicates an increase (decrease) in the percentage of the seasonal hazard intensity compared to the seasonal average.

Finally, using these results, we established a multihazard criteria. This criterion identifies locations where the modulator changes the seasonal pattern of single or multiple hazards (time-dependent with a modulator impacted a singles hazard) and multiple locations where regions exhibit the same response.

For simplification, we focused on the seasons when larger anomalies were observed during positive phases, specifically during the coldest season in each hemisphere (JJA for the SAM, DJF for the AO, and DJF for the ENSO). The results for negative phases can found in Supplementary Information (Fig S7-15).

Modulator-multiple hazards

El Niño-Southern Oscillation (ENSO)

While temporal dependency results were obtained at the municipal level, encompassing the national and local scales, Figs. 2, 3 show the national-scale results to maintain the global context. The results for $ENSO^{+}$ (DJF) revealed the following patterns: in the northeast Pacific, swell (W) was enhanced, affecting the American coast from Canada (+ 2%) to Peru (+ 1%), with the largest anomalies observed on the western coast of Mexico (up to + 28.8%) (Supplementary Fig. 1). Conversely, in the northwest Pacific, wind-sea (W) and swell (W) decreased in Japan (−2% for both parameters), Indonesia (−5%; −3%) and Australia (−3% for swell). In the Southern Ocean, wind and wave (W) increased at lower latitudes, with swell (W) intensification recorded on the coast of South Africa (+ 1%) (Supplementary Fig. S1). Wind-sea (S) intensified on the coasts of Fiji and Ecuador (+ 8% in both

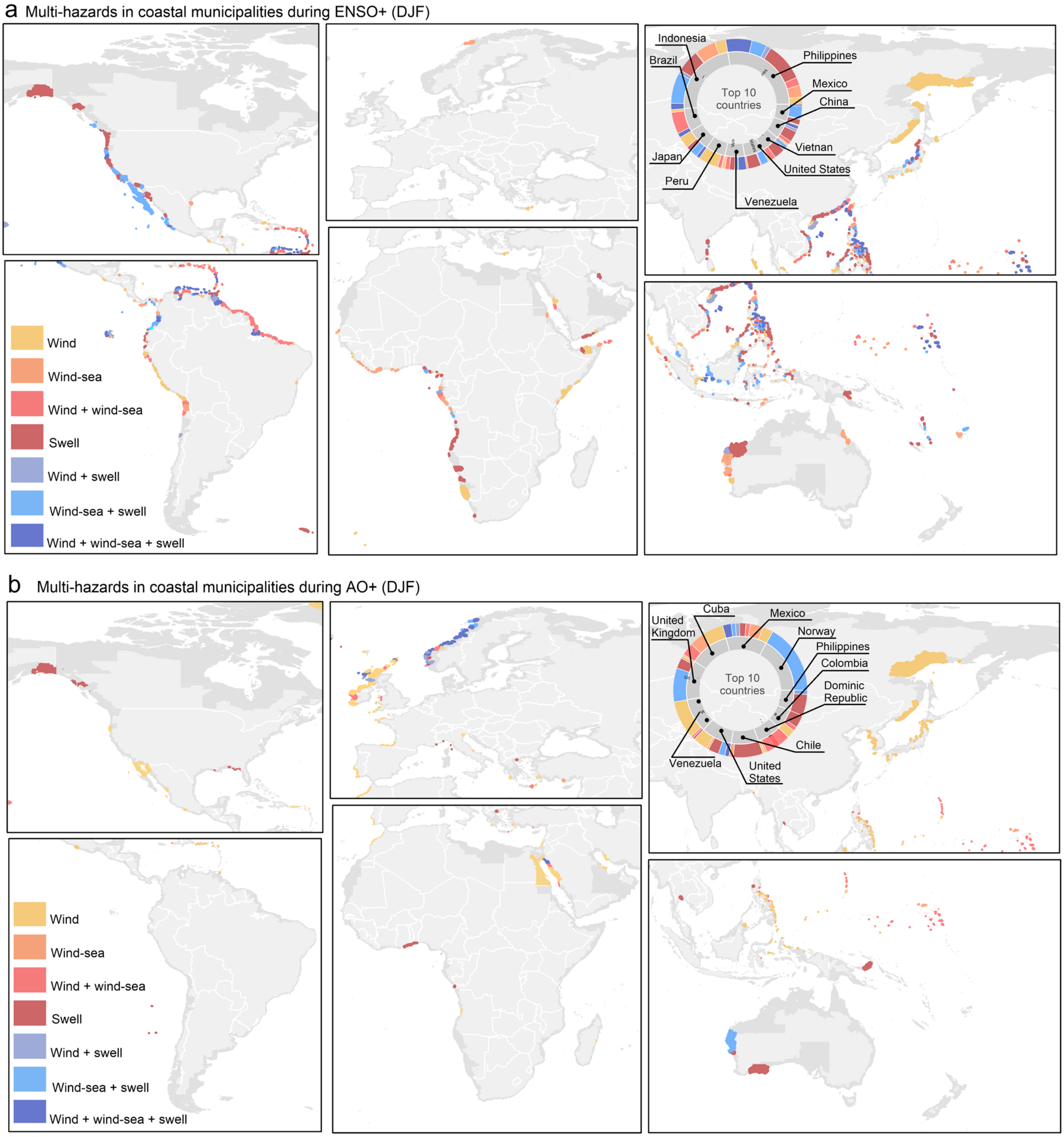

Figure 2. Regions impacted by long-term multihazards variability. (**a**) Municipalities affected by multihazards during El Niño (ENSO+) in the boreal winter (DJF). (**b**) Municipalities affected by multihazards during AO+ in the boreal winter (DJF).

areas), while wind-sea and swell (S) increased on the coasts of French Polynesia (+4%; +2%) (Supplementary Fig. S1).

In the northern tropical Pacific, wind (E) and wind-sea (E) increased on Pacific islands such as the Philippines (+1%; +1%), Indonesia (+1%; +6%), Fiji (+2%; +7%), Kiribati (+1%; +5%), the Marshall Islands (+1%; +2%) and Vanuatu (+4%). Tonga (+6%) experienced an increase in wind-sea (E) only. Anomalies of swell (E) also affected Pacific islands (Papua New Guinea, Fiji, Tonga, Tuvalu, Nauru, Vanuatu, and Malaysia), with an increase of +2%, while in Indonesia, swell (E) increased by up to +7% (Supplementary Fig. S1). Wind (E) decreased on the coasts of the Philippines (−5%), Australia (−4.5%), Vietnam (−5%) and the Paracel Islands (−3%) (Supplementary Fig. S1). In the western Pacific, wind-sea (E) decreased in Vietnam (−5%), the Paracel Islands (−3%) and the Philippines (−4.5%), and swell (E) decreased in Vietnam (−2%) and the Philippines (−2%) (Supplementary Fig. S1). In the Atlantic Ocean (Supplementary Fig. S1), wind (−0.5%) and wind-sea (E) (−3%) decreased on the a Multi-hazards in coastal municipalities during SAM+ (JJA)

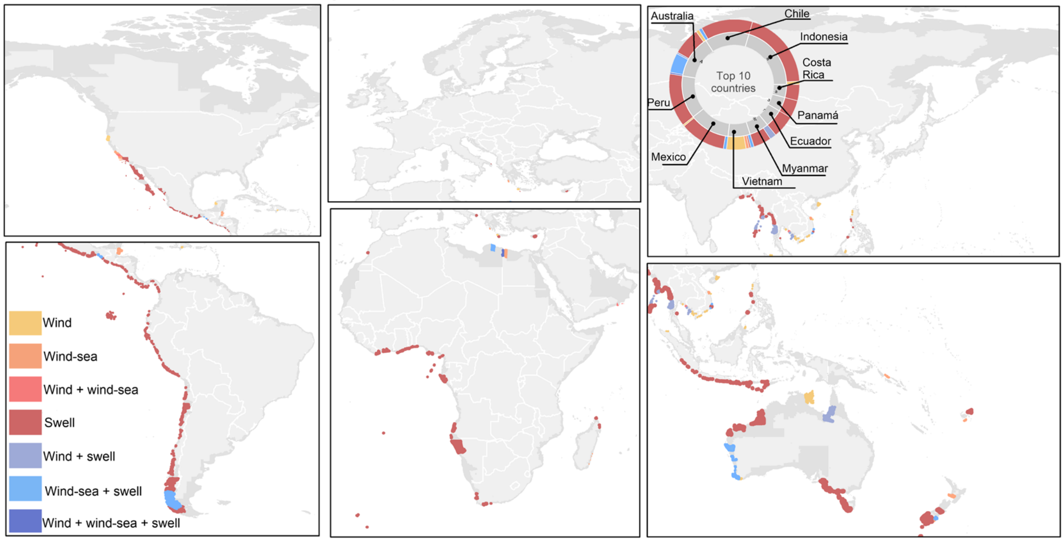

a Top 5 countries with the highest number of municipalities impacted by season and mode of natural climate variability

Season / mode	Country	Number of municipalities impacted per country						
		wind	wind-sea	wind wind-sea	swell	wind swell	wind-sea swell	wind wind-sea swell
ENSO+(DJF)	Philippines	8	13	9	43	5	17	29
	Indonesia	12	23	1	25	4	34	7
	Brazil	3		24				5
	Japan	13			6		8	4
	Peru	22		4	1			
ENSO+(MAM)	Indonesia	3	41	6		1	17	
	Brazil	3	1	29		1	1	7
	Philippines	7	6	3	12	1	2	2
	Peru	11	2	12			1	
	United States	3	1	11		1	1	2
ENSO+ (JJA)	Indonesia	84	26	32	19	4	32	44
	Brazil	3	8	29	2			12
	Chile	2	1	29		1		
	Venezuela	2		11	2	1		12
	Papua New Guinea	4	3	4	5		5	5
ENSO+ (SON)	Indonesia	17	23	2	11		7	2
	Solomon Islands	5			5		22	
	Brazil	17		7	2			4
	Venezuela	3		12			3	7
	Papua New Guinea	7	3		1	2	5	2
AO+(DJF)	Norway						33	
	Mexico	5	6	2	3	2	2	4
	Cuba	10	7	6				
	United Kingdom	1	1		5		16	
	Venezuela	18		1	1			
SAM+(JJA)	Indonesia	2			49			
	Chile				32		2	
	Australia	2			17	1	12	1
	Peru				33			
	Mexico	1			28		2	

Figure 3. Regions impacted by long-term multihazards variability and countries with the highest number of affected municipalities. (**a**) Municipalities affected by multihazards during SAM + in the boreal summer (JJA). (b) Top 5 countries with the highest number of affected municipalities by season and climate mode.

coasts of Caribbean islands (e.g., Barbados, Dominica, Anguilla, Antigua, Barbuda, Cuba, Monserrat, St. Kitts and Nevis, Guadalupe, Martinique and Puerto Rico). In the southern tropical Atlantic, wind-sea (E) in Colombia (8%) and swell (E) in Venezuela (−1%) decreased (Supplementary Fig. S1).

Arctic oscillation

During the AO + phase (DJF), an increase in wind (W) was observed on the coasts of Ireland and the UK (+ 2%) (Supplementary Fig. S2). Moreover, a reduction in wind (E) was observed on the eastern coast of Russia (−2%).

Wind-sea (W) and swell (W) increased in Ireland (+ 11% and + 9%, respectively), Norway (+ 15% and + 9%, respectively) and the UK (+ 12% and + 8%, respectively) (Supplementary Fig. S2). Additionally, on the northern coast of Spain and west of France, swell (W) increased by + 4% above the seasonal average. In contrast, swell (W) decreased in Japan (−3%), North Korea and South Korea (−4%). Waves originating from the south were unaffected by this climate mode, except on the coast of Iceland, where higher levels of wind-sea and swell were observed (+ 4% and + 4%, respectively).

Across the northern tropical Atlantic belt, wind (E) exhibited anomalies of ~ + 1% in the Bahamas, Cuba, Dominica, Dominican Republic, Haiti, Puerto Rico and the Canary Islands (Spain). Wind-sea (E) and swell (E) showed anomalies of approximately ~ + 5% in the Caribbean Sea (Supplementary Fig. S2).

Southern annular mode (SAM)

During the SAM$^+$ phase (JJA), swell (W) (Supplementary Fig. S3) increased on the coasts of Chile (~ + 2%), southeastern Australia (~ + 2%), and New Zealand (~ + 2%), while it decreased in southwestern Australia (~ −2%), South Africa (~ −2%), and the Philippines (~ −4%). Therefore, the increase in extratropical wind-sea (W) and swell (S) affected countries in the eastern Pacific (Supplementary Fig. S3): Peru, Ecuador, Mexico, Panama, Guatemala, Costa Rica, and Nicaragua (+ 1.5%). In the southeast Atlantic and Indian Oceans, swell (S) decreased (Supplementary Fig. S3) by approximately −1.5% (Ghana, Angola, Namibia, Indonesia, Madagascar, and St. Helena).

Multiple locations

We identified regions where concurrent seasonal anomalies of multiple hazards occurred under the influence of climate modes. Given that the dependencies and interactions between multiple hazards greatly depend on the spatial scale[30], we assessed two scales in this study: global and local.

In general, the ENSO (Fig. 2a) affected a larger number of coastal countries, reaching its maximum spatial influence during the colder seasons in each hemisphere (~ 38% of coastal countries in JJA and ~ 44% of coastal countries in DJF). Along with the SAM, Europe was the least impacted by the ENSO (Fig. 2a). In comparison, the AO (Fig. 2b) and SAM (Fig. 3a) affected approximately 30% of coastal countries.

The ENSO induced a greater diversity of multihazard combinations. While the AO and ENSO induced anomalies in both wind/wind-sea and wind/swell, the SAM did not significantly modify these pairwise anomalies but more notably influenced swells as a single hazard. This pattern is consistent with the considerable impact of this climate mode on the southern extratropical belts, where the most energetic swells develop and propagate towards the eastern coasts of the basins[6].

During all seasons, India and the Philippines exhibited the largest number of municipalities affected by El Niño, followed by countries on the American continent, such as Brazil, the USA, Chile, and Peru (Fig. 3b).

The SAM primarily affected countries such as Australia, China, Chile, and Indonesia, while the influence of the AO was greater in Norway, Mexico, the UK, Japan, and some countries located in the tropical Atlantic region, such as Cuba. While low-lying islands were not among the nations with the largest number of affected municipalities, some relevant results should be highlighted due to their high vulnerability to sea level rise[36]. During the ENSO + phase (DJF), trade winds exhibited complex patterns in the Pacific (Kiribati, the Paracel Islands, and the Philippines) and Atlantic (Cape Verde and Haiti), with variations of up to 5%, see Supplementary Information Fig. S4. The Pacific tropical islands (Fiji, Kiribati, the Marshall Islands, and Tonga) affected by wind-sea (E) exhibited variations of up to 17%, and swell (E) in the Marshall Islands, Tonga, and Vanuatu exhibited variations of up to 5%.

During the AO + phase (DJF), tropical Atlantic islands such as Cuba and Puerto Rico experienced wind (E) variations of up to 3% and swell variations of up to 5%. During the ENSO + phase (JJA), wind-sea on Papua New Guinea fluctuated by up to 15% (E) and 25% (S), and wind (S) varied by up to 10%. The combinations of hazards affecting islands varied with season and climate mode: some experienced a single hazard (e.g., Vanuatu and New Caledonia), while others faced multiple hazards (e.g., Papua New Guinea, Dominica and Martinique).

Regarding the negative phases, while the dynamics and physics can be explained as opposite behaviors, the results change the panorama completely in terms of the regions affected by coastal multihazards. For instance, during La Niña, global teleconnected SLP anomalies are inverted with respect to El Niño events[37]. During this phase, the regions most affected by multihazards are found in the Southern Hemisphere. Different phases can completely change the pairwise interactions and alter their spatial patterns.

Discussion

Our study revealed hazard patterns that align with those identified in previous studies focusing on wave[5,6,8] and wind dynamics[4]. Several studies have focused on analysing the effect of natural variability on single coastal hazards. However, these studies targeted specific regions heterogeneously distributed in space. At the global scale, detecting dependencies between hazards over time and space is complex, requiring the integration of the spatiotemporal variations in hazards and governing competencies in risk management across different regions. In this study, the global effects of climate modes on the seasonal intensity of concurrent hazards and their spatial variations were identified. While our focus is on winds and waves, it is important to note that other significant coastal hazards, such as river discharge, are not considered in this study. Additionally, an analysis was conducted at national and municipal levels, encompassing administration units with coastal risk competencies. The analysis provides a wide range of possibilities for interpretation and implementation by coastal practitioners.

Physical links with climate modes and multihazards

Our results are in line with previous studies related to the interannual variability of single hazards. The findings show that El Niño is the climate mode that most influences seasonal changes in multiple hazards. This is consistent with the anomaly patterns detected by other authors in winds and waves. In the tropical Pacific, where multihazards are compounded by winds, the trade winds weaken or even reverse[38]. Consistent with earlier works[11,39,40], in the North Pacific, ENSO + modifies extratropical waves in the Pacific region, where multihazards in the Northeast Pacific are caused by waves, both swells and wind-sea. El Niño induces a decrease in wave power in the Chilean coast by creating blocking high-pressure systems in this region[41] which, in comparison with La Niña, increase the wave power in the south of Chile. These results are captured by our multihazard analysis.

The AO is characterized by an increase in sea level pressure in high latitudes and a decrease in mid-latitudes in the Northern Hemisphere[42]. In the North Atlantic, during DJF under the positive phase of the AO, winds and wave energy intensify in high latitudes and decrease in mid-latitudes[43], affecting countries such as the UK, Norway, and the south of Iceland[12,44] as identified by multihazard analysis. Although the Pacific exhibits a weaker variation in signal induced by this climate mode than the Atlantic[42], our results show a significant impact on winds in the Northwest Pacific. The AO is known to influence the tropical belt of the Atlantic, which is significantly affected by multihazard combined wind and wind-sea. However, the results related to the Southern Hemisphere do not have a clear physical explanation due to the undemonstrated teleconnection between the hemispheres. Nonetheless, there could be some synchronization[45] that leads to significant results.

Both the AO and ENSO control tropical cyclone activity[46], which can modify the seasonal average of winds in the North Atlantic. In this study, in the tropical Atlantic, anomalies induced by these climate modes has been detected for both winds and waves propagating from the east for both climate modes.

The SAM modulates winds and waves in the extratropical belt of the Southern Hemisphere[6,8,47]. However, during the positive phase of SAM, westerlies are intensified in high latitudes of the Southern Hemisphere, but they do not reach the coasts[48]. Consequently, the results related to multihazard in coastal areas show variations only in the seasonal average of swell wave power, which aligns with previous studies[5,40].

Interaction of scales within the multihazard dependencies

The episodic cases shown in the Fig. 1 and described in the Supplementary Information can be explained using the proposed seasonal analysis approach.

Although this study did not focus on individual extreme events and acknowledges differences in the order of magnitude between synoptic events and seasonal averages, seasonal anomalies could encompass extreme events and capture patterns that may influence the intensity and seasonal probability distribution of storms[49]. We recognize that this can be perceived as a limitation of this study. However, the seasonal scale is important for risk response formulation, providing a practical approach to reduce the existing gap between disaster independence (hours), considered by the insurance industry, and the recovery period (years) for a given distaster[30].

Interannual anomalies influenced by climate modes can dominate seasonal conditions. This study quantifies these variations on different coastal hazards that can help towards the inclusion of climate modes as predictor in multihazards and distinguish where, geographically, to include them, or not. Contributing to the use of climate modes as seasonal predicants in coastal multihazards, in the same way it has been done for coastal sea level[16]. Interannual variations within seasons are influenced by climate modes, and seasonal warning systems have been implemented in different fields such as agriculture[50,51] and fisheries[52,53], primarily focused on the ENSO. These systems are instrumental for disaster risk reduction and contribute to improving planning in response to long-term climate variability.

However, such forecasts have yet to be implemented for multiple hazards in coastal areas. Seasonal forecasts of winds and waves could support annual decision-making processes in coastal planning, aiding in the prevention of critical structural damage and operability caused by co-occurring hazards.

Dependencies were comprehensively examined to synthesize the complex relationship between the long-term natural variability and seasonal variations from the global to local scales. In recent years, given the complexity of defining a multihazard event, several frameworks have been developed to facilitate understanding and assessment (e.g., Zscheischler et al.[28], Tilloy et al.[35], Gill and Malumud et al.[33]). To identify multihazard patterns induced by climate modes at the national and municipal levels, we refrained from using a specific typology and instead considered temporal, spatial, and related-element dependencies. We understand that the combination of these dependencies serves as a guideline for identifying multihazard types in any existing framework. Clearly, the next step will involve exploring the nature and typology of multiple hazards that can arise from climate modes at synoptic temporal scale, such as consecutive (a succession of storms), dependent (such as wind and wind-sea), and independent (wind and swell) hazards, to assess the joint likelihood of co-occurrence events and the induced risk. Additionally, we believe that the recovery time after a disaster is a dependency not yet integrated into multihazard classification.

Spatial scales are often more challenging to discern than temporal scales. At a single location, it is easier to understand the times and agents involved in post-disaster scenarios compared to analysing multiple locations, whether the economic, governmental, or transportation systems are part of a network. For instance, as noted by Ruiter et al.[30], when hazards co-occur at a distant location, they are assessed as consecutive events at the national level but are treated as a single hazard at each affected location. Conversely, if economic activity is relocated to an unaffected locality, the resulting consequences affect the local scale, while the economy of the country remains balanced[30]. Considering several administration levels, as was done in this study, could facilitate discerning multiregional interactions, although further research is needed to better understand the linkages with governance, tourism, maritime transport and coastal urban networks.

Relevance of the natural variability in attribution studies of coastal impacts

Attribution studies are critical for analysing climate change consequences, as they provide a criterion for distinguishing the relative contributions of different drivers to damage[30]. Natural variability is critical for such attribution analysis, as it can mask emerging global warming trends in areas characterized by substantial natural fluctuations, such as the Southern Ocean[6,54]. In this study, we identified whether long-term natural variability should be considered. For example, the sequence of storms during the 2013–2014 winter season was influenced in part by climate modes and climate change[26]. Nevertheless, these studies require holistic case-by-case studies and further research to explore the interplay between the long-term natural variability and climate change at the regional or global scale.

According to the results, the uncertainty in some regions is relatively high (Supplementary Fig. S4), exhibiting changes in magnitude and even in sign from one event to another. These changes are likely induced by shifts in the characteristics of the climate modes, which can create a barrier for multirisk assessment. A higher variance in mode-induced hazards was observed for the ENSO than for the polar climate modes (AO and SAM). This finding is consistent with the existing knowledge of the complexity of the ENSO; its magnitude, amplitude, and skewness render its predictability and modelling challenging, in contrast to annular modes, which exhibit more stable behaviour[10]. Moreover, for short-term projections (less than 15 years), the natural variability is the major source of uncertainty in climate predictions[55,56]. In future projections, despite improvements in the observed variability and characterization of the initial state[57], climate simulations do not perfectly replicate the sequence of climate modes, which is very important for shoreline evolution and requires an accurate climatic chronology. Additionally, it is acknowledged that climate modes respond to greenhouse gases, but there is a limited ability to quantify their responses[82].

Conclusions

Climate modes have been recognized as critical long-term drivers affecting seasonal waves[39] and wind conditions[23], thereby influencing multiple hazards and their consequences for coastal erosion[58] and impacting wind energy investment[23]. Nevertheless, until now, the causal links between climate modes and multiple hazards in coastal areas have not been established globally. This study focused on the local and global scales to facilitate the tracking of the complex interactions between hazards and consequences on different scales.

We emphasize that natural climate variability modes should be recognized as modulators of multiple hazards in coastal regions. Among the three leading climate modes analysed in this study, the ENSO is the climate driver causing the greatest disturbances in multiple hazards, affecting winds and waves in a pairwise manner in coastal areas worldwide, except Europe. Swells, which are related to flooding events, exhibit seasonal anomalies in the boreal summer during the positive phase of the SAM and in the boreal winter during El Niño. These findings are particularly important for low-lying islands, where waves play a crucial role in flooding events.

Methods

The proposed methodology aims to analyse the variability of climate modes on wind and wave hazards and to categorize municipalities based on the concurrent seasonal anomalies of multiple hazards. We first classified the hazards based on climates (Fig. 4a) which they belong— defined as the regions in the global oceans with similar characteristics, wave power and direction for waves and wind speed and direction for winds. This results into westerlies, easterlies and southerlies climates for both winds and waves. Second, we have identified the seasonal anomalies of each variable induced by a climate mode (Fig. 4b). With these results we applied a multihazard criteria (Fig. 4c). A detailed description of the method is provided and shown in Fig. 4.

Data

ERA5 near-surface winds and ocean wave parameters[59], for which the global performance of the seasonal and interannual variabilities has been widely validated[11,60]. The parameters of the near-surface wind speed (U_{10}), wind direction (Dir_w), wave direction (Dir_m) and wave power (P_w) were used. The wave power of irregular waves was obtained from the spectral energy density function expressed as $Pw = \frac{\rho g^2}{64\pi} T_e H_{m0}{}^2$, where the energy period is a function of the spectral mean period $T_e = \frac{m_{-1}}{m_0} = \alpha T_{01}$, with $\alpha = 1.08$[61]. Regarding the total wave power (P_w), we used the wave height of combined wind-sea waves and swells (H_{m0}) and the mean wave period T_{01}. Regarding the swell-wave power, we used the height ($H_{m0\text{-}sw}$) and wave period ($T_{01\text{-}sw}$) of swells. Regarding the wind-sea wave power, we used the height ($H_{m0\text{-}ww}$) and mean wave period ($T_{01\text{-}ww}$) of wind-sea waves.

The positive phases (expressed as $ENSO^+$, AO^+, and SAM^+) and negative phases (expressed as $ENSO^-$, AO^-, and SAM^-, respectively) of the climate modes were identified by using climate indices of the National Weather Service Climate Prediction Centre of the National Oceanographic and Administration (NOAA), namely, the AO (monthly AO index), SAM (monthly SAM index), and ENSO (multivariate ENSO index version 2, MEI.v2). For the AO and SAM, the positive/negative phases were defined by values above/lower than the average plus/minus the standard deviation ($\mu \pm \sigma$) of each index, while for El Niño, the positive phases of the ENSO were identified as MEIv2 ≥ 0.5, and for La Niña, the negative phase of the ENSO was identified as MEIv2 ≤ -0.5.

Hazard classification into climates.

Global winds and waves from 1979 to 2018 were classified using a dynamic clustering algorithm[6]. The advantages of using this "dynamic clustering" in multihazad analysis are that it identifies the similarities between spatially and temporally neighbouring data and tracks and relates climate data with similar variability. This method, without applying a dimensionality reduction, identifies similar waves and winds that are separated geographical areas driven by atmosphere dynamics. These characteristics show some advantages for detecting long-term variability in multihazards compared to common approaches. For instance, correlation analysis (implemented in other

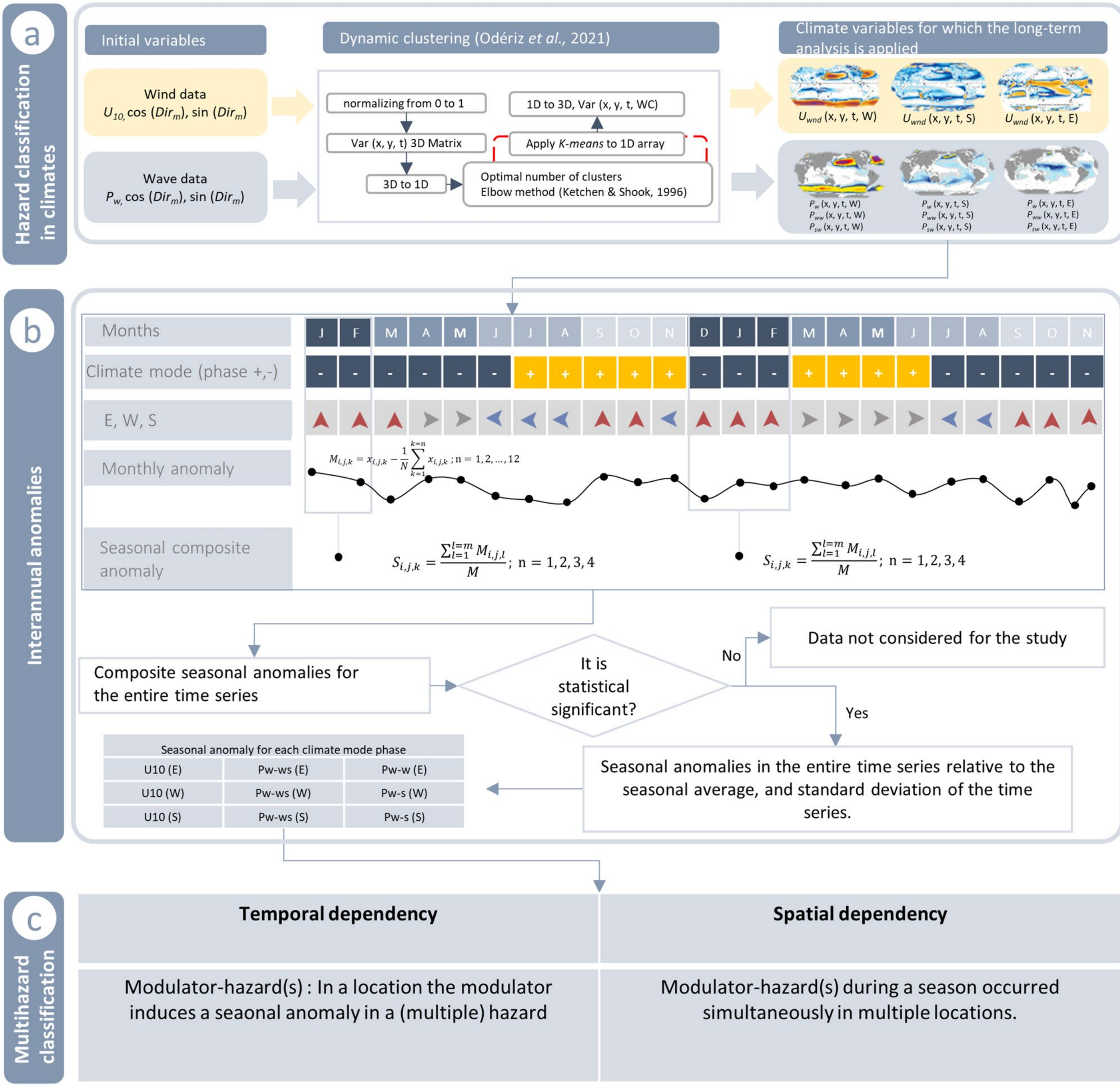

Figure 4. Overall view of the proposed methodology.

studies for single hazard[6,11,39]) is insufficient for quantifying the amplitude magnitude and describing spatial dependency[62,63], while time dependency is not well detected when empirical orthogonal functions are applied (implemented in other studies for single studies[5,44]). Following, a brief explanation of the global spatiotemporal classification of winds and waves is provided, but for further details, readers are referred to Odériz et al.[6].

The input monthly variables for winds were the wind speed (U_{10}) and directional components cos(Dir_w) and sin(Dir_w). For ocean waves, the variables chosen were the wave power for irregular waves (P_w) and directional components (cos(Dir_m) and sin(Dir_m)). The dynamic clustering algorithm[6] was applied separately for winds and waves and consisted of (i) normalizing the variables from 0 to 1; (ii) building an input matrix, which was reshaped from a 3D matrix (longitude, latitude, and time) to a 1D array; (iii) applying the K-means clustering algorithm[64] and elbow method[65] to identify the optimal number of clusters; and finally, (iv) reshaping the classification from a 1D array to a 3D array.

This resulted in a series of spatiotemporal indicators to identify waves and winds parameters (P_w and Dir_m; U_{10} and Dir_w) classified by westerlies, southerlies and easterlies winds and waves. In this paper, they are referred as W, S and E, respectively.

Interannual anomalies

This analysis focused only on the offshore points closest to coasts. Interannual anomalies of wind and wave climate conditions were addressed by computing composite anomalies (Fig. 1b). First, for each wind and wave climate (E, S and W), monthly anomalies ($A_{i,j}$) of the wind speed (U_{10}), total wave power (P_w), wind-sea wave power ($P_{w\text{-}ws}$), and swell wave power ($P_{w\text{-}s}$) were calculated as the monthly values for each year minus the corresponding monthly value averaged over all the years considered (1979–2018). The seasons were designated as follows: DJF for December, January and February; MAM for March, April and May; JJA for July, June and August; and SON for September, October and November.

Then, the composite anomalies for each season were calculated as the average of the monthly anomalies for a season, climate, and variable $J_{i,j,k} = \frac{\sum_{k=1}^{k=n} A_{i,j,k}}{n}$. With these seasonal composite anomalies, we calculate the average of all the values of seasonal composite anomalies and test their significance. The statistical significance of the composite anomalies was calculated using a two-tailed Student's t test at the 95% confidence level, with the null hypothesis of $H_0 : \mu_1 = \mu_2$ and the alternative hypothesis of $H_1 : \mu_1 \neq \mu_2$, and being the test statistic $T = \frac{\overline{X}_2 - \mu}{\sigma/\sqrt{n}}$ following the indications of Odériz et al.[6] Only composed anomalies that met the statistical test at the 95% confidence level were considered.

Then, to capture how much the phase of each climate mode perturbs seasonal winds and wave climatology, the percentage of the seasonal composite anomalies respect to the seasonal average was calculated. The study is able to identify variability in seasonal average conditions of 1%. The standard deviation of the seasonal composite anomalies was calculated to assess the uncertainty of the results.

Multiple hazards

Once we identified the influences of climate modes and hazard temporal dependencies, we categorized the municipalities based on the number of concurrent seasonal anomalies of multiple hazards. The spatial scale is critical when assessing multiple hazards because impacts can occur at the local scale, but their consequences can extend to larger areas. Furthermore, the results were provided at two administration levels: the national and municipal levels. To enable an understanding between spatial scales of climate modes and multiple hazards, the analysis is assessed at various administrative levels, national and municipal. Coastal municipality were selected from the GARDM data (version 4.0, https://gadm.org/). For this, the analysis was focusing only on the offshore points closest to coasts to the centroid of each municipality.

The municipalities were classified based on the following categories:

Modulator—single hazard

A climate mode induces a seasonal anomaly in a single hazard (wind, swell or wind-sea). These are time-dependent, as the climate mode induces a seasonal anomaly that can translate into changes in storminess and/or average conditions of the season.

Modulator—multiple hazards

A climate mode induces a seasonal anomaly in multiple hazards (wind and wind-sea; wind and swell; wind-sea and swell; wind, wind-sea, and swell.). The same time-dependent criteria apply, except the climate mode induces anomalies in several hazards.

Multiple locations

Regions affected under a season and a climate mode that are impacted by the first and second multihazard.

Data availability

Wave and wind data are sourced from the Copernicus Services (https://cds.climate.copernicus.eu/cdsapp#!/dataset/reanalysis-era5-single-levels?tab=overview). The climate index is obtained from NOAA (https://psl.noaa.gov/data/climateindices/list/). The coastal municipalities data is based on information provided by GADM (https://gadm.org/). All the data reported in the main text and supplementary information are available at the repository Zenodo with DOI https://doi.org/10.5281/zenodo.8406271.

Code availability

The figures were generated with Python, surfer (Golden Software) and ArcMap. Routines are available upon request from the corresponding author I.O.

Received: 7 March 2024; Accepted: 15 July 2024
Published online: 23 July 2024

References

1. Bertrand, J. L. & Brusset, X. Managing the financial consequences of weather variability. *J. Asset. Manag.* **19**, 301–315 (2018).
2. Lazo, J. K., Lawson, M., Larsen, P. H. & Waldman, D. M. U. S. Economic sensitivity to weather variability. *Bull. Am. Meteorol. Soc.* **92**, 709–720 (2011).
3. Smith, S. C. & Ubilava, D. The El Niño Southern Oscillation and economic growth in the developing world. *Glob. Environ. Chang.* **45**, 151–164 (2017).
4. Freitas, A., Bernardino, M. & Guedes Soares, C. The influence of the Arctic Oscillation on North Atlantic wind and wave climate by the end of the 21st century. *Ocean Eng.* https://doi.org/10.1016/j.oceaneng.2022.110634 (2022).
5. Echevarria, E. R., Hemer, M. A., Holbrook, N. J. & Marshall, A. G. Influence of the Pacific-South American modes on the global spectral wind-wave climate. *J. Geophys. Res. Oceans* **125**, e2020JC016354 (2020).
6. Odériz, I. *et al.* Natural variability and warming signals in global ocean wave climates. *Geophys. Res. Lett.* **48**, e2021GL093622 (2021).
7. Odériz, I., Silva, R., Mortlock, T. R. & Mori, N. El Niño-Southern oscillation impacts on global wave climate and potential coastal hazards. *J. Geophys. Res. Oceans* https://doi.org/10.1029/2020JC016464 (2020).

8. Hemer, M. A., Church, J. A. & Hunter, J. R. Variability and trends in the directional wave climate of the Southern Hemisphere. *Int. J. Climatol.* **30**, 475–491 (2010).
9. Reguero, B. G., Losada, I. J. & Méndez, F. J. A recent increase in global wave power as a consequence of oceanic warming. *Nat. Commun.* **10**, 1–14 (2019).
10. Timmermann, A. *et al.* El Niño-Southern Oscillation complexity. *Nature* **559**, 535–545. https://doi.org/10.1038/s41586-018-0252-6 (2018).
11. Odériz, I., Silva, R., Mortlock, T. R. & Mori, N. ENSO Impacts on Global Wave Climate and Potential Coastal Hazards. *J. Geophys. Res. Oceans* **125**, e2020JC016464 (2020).
12. Izaguirre, C., Méndez, F. J., Menéndez, M. & Losada, I. J. Global extreme wave height variability based on satellite data. *Geophys. Res. Lett.* **38**, 1–6 (2011).
13. Adam, E. F., Brown, S., Nicholls, R. J. & Tsimplis, M. A systematic assessment of maritime disruptions affecting UK ports, coastal areas and surrounding seas from 1950 to 2014. *Nat. Hazards* **83**, 691–713 (2016).
14. Nelson, V. *Wind Energy* (CRC Press, 2009). https://doi.org/10.1201/9781420075694.
15. Gliksman, D. *et al.* Review article: A European perspective on wind and storm damage - from the meteorological background to index-based approaches to assess impacts. *Nat. Hazards Earth Sys. Sci.* **23**, 2171–2201. https://doi.org/10.5194/nhess-23-2171-2023 (2023).
16. Boucharel, J., David, M., Almar, R. & Melet, A. Contrasted influence of climate modes teleconnections to the interannual variability of coastal sea level components–implications for statistical forecasts. *Clim. Dyn.* **61**, 4011–4032 (2023).
17. Toimil, A. *et al.* Climate change-driven coastal erosion modelling in temperate sandy beaches: Methods and uncertainty treatment. *Earth Sci. Rev.* **202**, 103110 (2020).
18. Vetter, O. *et al.* Wave setup over a Pacific Island fringing reef. *J. Geophys. Res. Oceans* https://doi.org/10.1029/2010JC006455 (2010).
19. Amoudry, L. O. & Souza, A. J. Deterministic coastal morphological and sediment transport modeling: A review and discussion. *Rev. Geophys.* https://doi.org/10.1029/2010RG000341 (2011).
20. van Gent, M. R. A. Influence of oblique wave attack on wave overtopping at caisson breakwaters with sea and swell conditions. *Coast. Eng.* https://doi.org/10.1016/j.coastaleng.2020.103834 (2021).
21. Romano-Moreno, E., Diaz-Hernandez, G., Tomás, A. & Lara, J. L. Multimodal harbor wave climate characterization based on wave agitation spectral types. *Coast. Eng.* https://doi.org/10.1016/j.coastaleng.2022.104271 (2023).
22. Muis, S., Haigh, I. D., Guimarães Nobre, G., Aerts, J. C. J. H. & Ward, P. J. Influence of El Niño-Southern oscillation on global coastal flooding. *Earths Futur.* **6**, 1311–1322 (2018).
23. Kirchner-Bossi, N., García-Herrera, R., Prieto, L. & Trigo, R. M. A long-term perspective of wind power output variability. *Int. J. Climatol.* **35**, 2635–2646 (2015).
24. Kamranzad, B., Amarouche, K. & Akpinar, A. Linking the long-term variability in global wave energy to swell climate and redefining suitable coasts for energy exploitation. *Sci. Rep.* https://doi.org/10.1038/s41598-022-18935-w (2022).
25. Little, A. S., Priestley, M. D. K. & Catto, J. L. Future increased risk from extratropical windstorms in northern Europe. *Nat. Commun.* https://doi.org/10.1038/s41467-023-40102-6 (2023).
26. Schaller, N. *et al.* Human influence on climate in the 2014 southern England winter floods and their impacts. *Nat. Clim. Chang.* **6**, 627–634 (2016).
27. Turner, I. L. *et al.* A multi-decade dataset of monthly beach profile surveys and inshore wave forcing at Narrabeen, Australia. *Sci. Data* https://doi.org/10.1038/sdata.2016.24 (2016).
28. Zscheischler, J. *et al.* A typology of compound weather and climate events. *Nat. Rev. Earth Environ.* **1**, 333–347. https://doi.org/10.1038/s43017-020-0060-z (2020).
29. United Nations Office for Disaster Risk Reduction (UNDRR). *Sendai Framework for Disaster Risk Reduction 2015–2030* (2015).
30. de Ruiter, M. C. *et al.* Why We Can No Longer Ignore Consecutive Disasters. *Earth Futur.* https://doi.org/10.1029/2019EF001425 (2020).
31. Hurrell, J. W., Kushnir, Y., Ottersen, G. & Visbeck, M. An Overview of the North Atlantic Oscillation. In *The North Atlantic Oscillation: Climatic Significance and Environmental Impact* (eds Hurrell, James W. *et al.*) 1–35 (American Geophysical Union, 2003).
32. Yeo, S. R. & Kim, K. Y. Decadal changes in the Southern Hemisphere sea surface temperature in association with El Niño-Southern oscillation and Southern annular mode. *Clim. Dyn.* **45**, 3227–3242 (2015).
33. Gill, J. C. & Malamud, B. D. Reviewing and visualizing the interactions of natural hazards. *Rev. Geophys.* **52**, 680–722. https://doi.org/10.1002/2013RG000445 (2014).
34. Claassen, J. N. *et al.* A new method to compile global multi-hazard event sets. *Sci. Rep.* **13**, 13808 (2023).
35. Tilloy, A., Malamud, B. D., Winter, H. & Joly-Laugel, A. A review of quantification methodologies for multi-hazard interrelationships. *Earth Sci. Rev.* https://doi.org/10.1016/j.earscirev.2019.102881 (2019).
36. Mycoo, M. *et al. SPM Small Islands to the Sixth Assessment Report of the Intergovernmental Panel on Climate Change* 2043–2121 (Cambridge University Press, 2022).
37. Wang, B., Wu, R. & Fu, X. Pacific-East asian teleconnection: How does ENSO affect East Asian Climate?. *J. Clim.* **13**, 1517–1536 (2000).
38. Wang, H., Kumar, A., Wang, W. & Xue, Y. Influence of ENSO on pacific decadal variability: An analysis based on the NCEP climate forecast system. *J Clim* **25**, 6136–6151 (2012).
39. Reguero, B. G., Losada, I. J. & Méndez, F. J. A global wave power resource and its seasonal, interannual and long-term variability. *Appl. Energ.* **148**, 366–380 (2015).
40. Sardana, D. & KumarRajni, P. Influence of climate variability modes over wind-sea and swell generated wave energy. *Ocean Eng.* **291**, 116471 (2024).
41. Fogt, R. L. & Bromwich, D. H. Decadal variability of the ENSO teleconnection to the high-latitude South Pacific governed by coupling with the Southern Annular Mode. *J. Clim.* **19**, 979–997 (2006).
42. Deser, C. On the teleconnectivity of the 'Arctic Oscillation'. *Geophys. Res. Lett* **27**, 779–782 (2000).
43. Freitas, A., Bernardino, M. & Guedes Soares, C. The influence of the Arctic Oscillation on North Atlantic wind and wave climate by the end of the 21st century. *Ocean Eng.* **246**, 110634 (2022).
44. Stopa, J. E. & Cheung, K. F. Periodicity and patterns of ocean wind and wave climate. *J. Geophys. Res. Oceans* **119**, 5563–5584 (2014).
45. Tachibana, Y. *et al.* Interhemispheric synchronization between the AO and the AAO. *Geophys. Res. Lett.* **45**, 13477–13484 (2018).
46. Larson, J. & Higgins, R. W. *Characteristics of Landfalling Tropical Cyclones in the United States and Mexico: Climatology and Interannual Variability*. www.cpc.ncep.noaa.gov/products/precip/realtime/ (2005).
47. Marshall, A. G., Hemer, M. A., Hendon, H. H. & McInnes, K. L. Southern annular mode impacts on global ocean surface waves. *Ocean Model (Oxf.)* **129**, 58–74 (2018).
48. Cai, W. Antarctic ozone depletion causes an intensification of the Southern Ocean super-gyre circulation. *Geophys. Res. Lett.* https://doi.org/10.1029/2005GL024911 (2006).
49. Smith, D. M., Scaife, A. A. & Kirtman, B. P. What is the current state of scientific knowledge with regard to seasonal and decadal forecasting?. *Environ. Res. Lett.* https://doi.org/10.1088/1748-9326/7/1/015602 (2012).
50. Anderson, W., Seager, R., Baethgen, W. & Cane, M. Trans-Pacific ENSO teleconnections pose a correlated risk to agriculture. *Agric. For. Meteorol.* **262**, 298–309 (2018).

51. Gelcer, E. *et al.* Influence of El Niño-Southern oscillation (ENSO) on agroclimatic zoning for tomato in Mozambique. *Agric. For. Meteorol.* **248**, 316–328 (2018).
52. Aguilera, S. E., Broad, K. & Pomeroy, C. Adaptive capacity of the monterey bay wetfish fisheries: Proactive responses to the 2015–16 El Niño event. *Soc. Nat. Resour.* **31**, 1338–1357 (2018).
53. Broad, K., Pfaff, A. S. P. & Glantz, M. H. Effective and equitable dissemination of seasonal-to-interannual climate forecasts: Policy implications from the peruvian fishery during El Niño.1997-98. *Clim. Chang.* **54**, 415–438 (2002).
54. Clem, K. R. *et al.* Record warming at the South Pole during the past three decades. *Nat. Clim. Chang.* **10**, 762–770 (2020).
55. Doblas-Reyes, F. J. *et al.* Initialized near-term regional climate change prediction. *Nat. Commun.* https://doi.org/10.1038/ncomms2704 (2013).
56. Blanusa, M. L., López-Zurita, C. J. & Rasp, S. Internal variability plays a dominant role in global climate projections of temperature and precipitation extremes. *Clim. Dyn.* https://doi.org/10.1007/s00382-023-06664-3 (2023).
57. Climate Change, I. P. C. C. *The Physical Science Basis Contribution of Working Group I to the Fifth Assessment Report of the Intergovernmental Panel on Climate Change* (Cambridge University Press, 2013).
58. Vos, K., Harley, M. D., Turner, I. L. & Splinter, K. D. Pacific shoreline erosion and accretion patterns controlled by El Niño/Southern Oscillation. *Nat. Geosci.* **16**, 140–146 (2023).
59. Hersbach, H. *et al.* The ERA5 global reanalysis. *Q. J. Royal Meteorol. Soc.* **146**, 1999–2049 (2020).
60. Timmermans, B. W., Gommenginger, C. P., Dodet, G. & Bidlot, J.-R. Global wave height trends and variability from new multimission satellite altimeter products, reanalyses, and wave buoys. *Geophys Res Lett.* **47**, e2019GL086880 (2020).
61. Webb, A. & Fox-Kemper, B. Impacts of wave spreading and multidirectional waves on estimating stokes drift. *Ocean Model (Oxf.)* **96**, 49–64 (2015).
62. Langenbrunner, B. & Neelin, J. D. Analyzing enso teleconnections in cmip models as a measure of model fidelity in simulating precipitation. *J. Clim.* **26**, 4431–4446 (2013).
63. Perry, S. J., McGregor, S., Sen Gupta, A., England, M. H. & Maher, N. Projected late 21st century changes to the regional impacts of the El Niño-Southern oscillation. *Clim. Dyn.* **54**, 395–412 (2020).
64. MacQueen, J. Some methods for classification and analysis of multivariate observations. in Proc*: of the Fifth Berkeley Symposium on Mathematical Statistics and Probability, Volume 1: Statistics* 281–297 (University of California Press, Berkeley, Calif., 1967).
65. Ketchen, D. J. & Shook, C. L. The application of cluster analysis in strategic management research: An analysis and critique. *Strategic Manag. J.* **17**, 441–458 (1996).

Acknowledgements

I.O. acknowledges the financial support through the Juan de La Cierva Programme FJC2021-047909-I, funded by MCIN/AEI/https://doi.org/10.13039/501100011033 and European Union (NextGenerationEU/PRTR). This study forms part of the ThinkInAzul programme and was supported by Ministerio de Ciencia e Innovación with funding from European Union NextGeneration EU (PRTR-C17.I1) and by Comunidad de Cantabria. It is also part of the FENIX Project funding by Comunidad de Cantabria.

Author contributions

I.O. and I.J.L conceived the study. I.O. lead the formal analysis and wrote the original draft of the manuscript. I.J.L. supervised the study and acquired the resources, I.O. and I.J.L. acquired the funding. All authors, investigated, discussed the results, reviewed and edited the manuscript.

Competing interests

The authors declare no competing interests.

Additional information

Supplementary Information The online version contains supplementary material available at https://doi.org/10.1038/s41598-024-67679-2.

Correspondence and requests for materials should be addressed to I.O.